

IMECE2019-10523

DESIGN RESILIENCE OF DEMAND RESPONSE SYSTEMS UTILIZING LOCALLY COMMUNICATING THERMOSTATICALLY CONTROLLED LOADS

Jason Kuwada

Mechanical & Biomedical Engineering
Boise State University
Boise, Idaho 83725
Email: jasonkuwada@gmail.com

Hoda Mehrpouyan

Computer Science
Boise State University
Boise, Idaho 83725
Email: hodamehrpouyan@boisestate.edu

John F Gardner*

Mechanical & Biomedical Engineering
Boise State University
Boise, Idaho 83725
Email: jgardner@boisestate.edu

ABSTRACT

Thermostatically Controlled Loads (TCLs) have shown great potential for Demand Response (DR) events. The focus of this study is to investigate the effects of adding communication throughout a population of TCLs on the resilience of the system. A Metric for resilience is calculated on varying populations of TCLs and verified with agent based modeling simulations. At the core of this study is an added thermostat criterion created from the combination of a proportional gain and the average compressor operating state of neighboring TCLs. Differing connection architectures are also analyzed. Resilience of the systems under different connection topologies, are calculated by analyzing algebraic connectivity at varying population sizes. The resilience analysis was verified through simulation. Results of the analysis show the effect of on delay schemes and connection architecture on stability limit of each system. Good concurrence was found between predicted and observed resilience for smaller dead-band sizes. Simulations showed varying results on the effect of a simulated attack based on location of the attack within the population.

1 INTRODUCTION

The rapid deployment of intermittent renewable energy generation on the electric grid has presented significant challenges to the entities that are responsible for maintaining the reliability of our electric distribution system. The challenges inherent

in this rapid expansion of renewables has been typified by the so-called “duck curve” first demonstrated by the California Independent System Operator (CAISO) [1]. The report highlights two significant challenges of widespread behind the meter solar deployment: steep ramp of demand at sunset, and over generation in mid-day. Some form of energy storage is cited as a solution to these problems, with grid-level batteries dominating the discussion.

But batteries are only one way to tame the duck curve. A growing number of energy observers are pointing out that by enlisting the cooperation of electricity users, and incentivizing changes in their behavior, we can impact the problem by changing consumption at critical times of the day [2]. Increasing development of the electrical smart grid offers unprecedented opportunity for more complex electrical supply and demand interactions in a relationship that has been historically unilateral. The smart grid allows for the application of modern communication technology, such as the internet of things, to improve or modify widespread electrical transmission and distribution.

Much of this activity is focused on thermostatically-controlled loads (TCLs) such as those systems used for space heating and cooling, hot water or refrigeration and food storage. Systems that use electricity in this manner are normally designed to maintain temperature, not at a single constant set point, but within a range of temperatures, known as the thermostat dead-band.

In a typical DR application, residential air conditioning (AC) compressors (but not the circulating fan) are temporarily turned

*Address all correspondence to this author.

off under control of the utility, allowing the inside temperature to rise above the thermostat setting. The grid is relieved of the load that the AC compressor would have drawn and the homeowner (if present) experiences a small and possibly noticeable increase in indoor temperature. These programs are nearly universally used to shed load at times of very high demand, but they can also be used to increase consumption at times of energy surplus, resulting in a somewhat cooler home than the set point would imply. A common interpretation of this effect is that energy is being stored in the thermal mass of the home. In this respect, the home acts like a thermal battery, albeit a leaky one with limited storage capacity.

The ability of any individual TCL to impact the energy balance of the grid is limited. Therefore, most applications entail the aggregation of many hundreds and thousands of loads, coordinated by a central controller. The dynamics and control of such aggregated loads is the subject of significant research [2], [3], [4] and grid operators across the country have significant experience using aggregated DR to manage peak loads.

2 Background

Grid operators typically exert central control over large populations of TCLs through radio links or power line carrier protocols. For example, Idaho Power has an AC Cool Credit program where individual consumers, in exchange for a small reduction in their monthly electric bill, give the utility permission to install equipment on their AC unit. This equipment can receive a signal from the grid operator that shuts off the unit's compressor for a short period of time. After that time has expired, the unit is allowed to turn back on while another population is disconnected, thus reducing the overall demand for as long as required and preventing uncomfortable conditions from occurring within any individual homes.

Another common method of controlling TCLs is through set-point control. Callaway [2] makes the case that changing thermostat set-points of a population of TCLs can be used to follow the variability of wind generation. Building on this work, Bashash and Fathy [5, 6] developed a model that uses a centralized controller to broadcast a uniform signal to vary the thermostat set-point temperature of the population of TCLs. This enables the tracking of a real wind power trajectory.

A centralized controller can coordinate many agents without knowing individual agent states. By comparing a reference to a received aggregate output value, the controller determines what signal to broadcast to all agents. Each agent then makes a decision based on the signal and defined probabilities [7].

Similarly, Zhang et al. [8] developed a control scheme where the centralized control signal is broadcast to all agents. The agents then decide how to implement the signal based on their local temperature and power state.

A priority-stack-based control strategy can be an effective

way to control TCLs [9]. Sorting the population of TCLs by temperature into two stacks, one where the TCLs are off and the other where the TCLs are on, allows for the most appropriate selection of the next TCL to turn on or off. When the grid has excess power, perhaps due to an increase in wind generation, the centralized controller can send a signal to the TCLs. The TCL with the highest priority in the off stack will turn on first and then continue down the stack until the excess power is being utilized. This also works the other way. When the grid is trying to reduce load, the TCLs in the on column turn off sequentially, in order of priority, until the desired reduction has been met. The downside of this model is the need to have the information of all agents in the system accessible to the central controller to sort correctly.

Other researchers have taken a more de-centralized approach. For example, using price signalling and adaptive mechanisms, coupled with smart meters, to prevent loads from syncing up and creating high peak demand [10].

With the rising number of electric vehicles (EVs), an additional opportunity for demand response has been created. EV charging management allows for the vehicles to charge at times of low demand or to match renewable energy production. Xydas et al. [11] developed a model to demonstrate the effectiveness of "responsive" EVs. These vehicles determine their charging schedule according to a signal that takes power demand and generation forecasts into account. Their model demonstrated that responsive EVs could reduce the peak charging demand of all EVs, including unresponsive EVs, by shifting demand to a time when the unresponsive EVs were finished charging. They also demonstrated the ability of responsive EVs to charge in response to a real time photovoltaic (PV) generation profile.

2.1 Security And Resilience

With more and more demand response being added to the power grid in efforts to mitigate over generation issues, issues of security and resilience begin to emerge. Security of cyber physical systems, such as the electric grid, have become a growing topic of interest. Need for security can be seen from examples such as the Ukraine Power Grid Attack [12]. In order to design, not only a secure system for demand response, but a secure and resilient system the definitions of both must be understood in terms of cyber physical systems.

Security, as defined by the US Department of Homeland Security, is the act of adding physical means or cyber defense measures to reduce the risk of a critical infrastructure [13]. These defenses protect from intrusions, attacks, or the effects of both natural and man-made disasters. Example provided for security measures include requiring badge entry at doors and using antivirus software. Through this definition and examples, it can be seen that security of cyber-physical systems work to keep unauthorized users, both intentional and unintentional, from accessing critical information and data from the system. If security is used

to keep unauthorized users out of a system, what can be done to reduce the effects of intruders who have successfully infiltrated the system?

Resilience offers systems the ability to endure and recover from attacks, intentional and unintentional, as well as naturally occurring threats. This is done through the effort to prepare and adjust to changing conditions and possessing the ability to recover from system disturbances. An example of a resilience measure is installing a generator to provide back up powering in the case of a power outage [14]. A deeper definition of resilience in terms of cyber-physical systems is provided by Rieger et al. through the definition of resilient control systems [15]. Rieger et al. defines resilient control systems as a system 'that maintains state awareness and an accepted level of operational normalcy in response to disturbances, including threats of an unexpected and malicious nature.

Rothrock explains the problem of relying solely on security is that security will not stop all attacks [14]. Because attacks are not always from outside adversaries and the security system cannot prepare for every possible attack, the system cannot be 'locked down' to the point where all attacks are defended against. Resilience is need for cyber physical systems in able to ensure operation amidst having the systems vulnerabilities exploited.

Vulnerabilities are security flaws and can be found in any system. Any vulnerability can be exploited by an adversary to become an entry point to the system. A common entry point in cyber physical systems is communication between devices and added communication is an integral component to demand response systems. While vulnerabilities of a system are inherently created through the design of the system, albeit generally created unintentionally, the ability to overcome system vulnerabilities can also be incorporated at early stages of the design stage.

Resilience itself is an emergent property of a system [16]. Therefore the resilience of a system can not only be analyzed by studying the interactions between individual parts of the system, but also be altered by changing those interactions. This means that the resilience of a demand response system can be improved through alterations of the communication used.

3 Modeling Approach

The core of this approach is a small amount of information sharing between thermostats that are in close proximity. For this study, thermostats allow each home to be aware of the on/off state of the compressors in the four nearest homes. The selection of the connections may be defined by the layout of the neighborhood (e.g. the next door neighbors, the house across the street and over the fence in the backyard) or they may be defined by the topology of the electric distribution system.

The logistics of information sharing are not covered in this study, but it is clear that a large number of options are available covering a spectrum of technologies from internet-based

server models where the connections can be implemented and programmed centrally, to local communication protocols such as Zigbee, Bluetooth and power-line carrier methods [17].

It is also important to address privacy concerns in information sharing situations. These concerns are addressed by noting that the information being shared (whether the compressor is on or off) is something a typical next door neighbor can observe by opening the window that is nearest the neighbor's outdoor condenser unit. In some locations, that information could be deduced from a careful observer on the public sidewalk. This information is likened to be similar to whether or not inside lights are on. While it is not usually noticed, it is clearly observable from the outside.

This work builds on the model first proposed by Malhamé and Chong [3]. Callaway furthers this work by contributing equivalent parameters for the first order model and showing populations of thermostatically controlled loads can act as virtual storage devices by collectively managing them [2]. Through this work, Callaway found load populations with greater heterogeneity are better candidates for set-point control of thermostatically controlled loads, where previous work focused on homogeneous populations. Bashash and Fathy modeled each thermostatically controlled load with their own first order differential equation and used Monté Carlo simulations to represent the community [5]. The analysis of this paper begins with the model proposed in that reference, shown below in Equation 1.

$$\dot{T} = \frac{1}{RC} \left(T_{\infty} - T(t) + R(Q_I - m(t)Q) \right) \quad (1)$$

where:

$T(t)$	Indoor Air Temperature	$^{\circ}\text{C}$
T_{∞}	Outdoor Air Temperature	$^{\circ}\text{C}$
C	Thermal Capacitance of Building	$\text{kWh}/^{\circ}\text{C}$
R	Thermal Resistance of Building	$^{\circ}\text{C}/\text{kW}$
Q_I	Internal Heat Gain	kW
Q	Load Cooling Capacity	kW
$m(t)$	Discrete State of AC Power	-

It should be noted that the variable $m(t)$ is a discrete variable representing the operating state of the air conditioning unit, having a value of one if the unit is operating and a value of zero if the unit is off. This is shown mathematically in Equation 2.

$$m(t) = \begin{cases} 0, & \text{if } T(t) \leq T_{min} \\ 1, & \text{if } T(t) \geq T_{max} \\ m(t^-), & \text{otherwise} \end{cases} \quad (2)$$

where T_{min} and T_{max} are the lower and upper limits of the thermostat deadband, δ . The setpoint temperature, T_{sp} , is related to these limits as shown in Equation 3.

$$T_{min} = T_{sp} - \frac{\delta}{2}, \quad T_{max} = T_{sp} + \frac{\delta}{2} \quad (3)$$

Considering a population containing N , number, of TCLs, the total load can be expressed as

$$P_{TCL}(t) = \sum_{i=1}^N \frac{1}{\eta_i} \bar{Q}_i m_i(t) \quad (4)$$

where η_i is the coefficient of performance (COP) of the i^{th} load.

Graph theory is the mathematical lens through which a network of connected houses can be viewed. Networks of connections are often represented as an adjacency matrix, \mathcal{A} . For a network containing N nodes, the adjacency matrix has N rows and N columns containing elements that follow the rules:

$$\mathcal{A}_{ij} = \begin{cases} 0, & \text{if nodes } i \text{ and } j \text{ are not connected to each other} \\ 1, & \text{if nodes } i \text{ and } j \text{ are connected to each other} \end{cases} \quad (5)$$

For an undirected network the adjacency matrix is symmetric, $\mathcal{A}_{ij} = \mathcal{A}_{ji}$, and since a house is not connected to itself, the diagonal consists of zeros. The adjacency matrix can be used to find the degree of house i by summing either the column or the row corresponding to that house:

$$d_i = \sum_{j=1}^N \mathcal{A}_{ij} = \sum_{j=1}^N \mathcal{A}_{ji} \quad (6)$$

Two graph topologies are considered here, the square lattice with periodic boundary conditions and the ring lattice. In both cases, the degree of the graph is 4, that is, each home is in communication with 4 nearby homes. These contrast with the star type graph which represents the case in which the grid operator directly controls each individual actor.

Now consider a situation in which the state of the AC unit, $m(t)$, for each house can be communicated from its thermostat to nearby connected thermostats. The variable \tilde{m}_i is introduced to represent the average state of the thermostats communicating with agent i . The adjacency matrix representing connected agents can be used to easily calculate all of these values simultaneously:

$$\tilde{\mathbf{m}} = \frac{1}{d} \mathcal{A} \mathbf{m} \quad (7)$$

In Equation 7, $\tilde{\mathbf{m}}$ and \mathbf{m} are vectors of N , number of homes, representing the entire population. \mathcal{A} is a matrix of $N \times N$ size, as defined as in Equation 5.

3.1 Modified Thermostat Behavior

Consider a new non-dimensional temperature variable defining a normalized position within the deadband, θ_i , where the bottom of the deadband is $\theta_i = 0$ and the top of the deadband is $\theta_i = 1$.

$$\theta_i = \frac{T_i - T_{min,i}}{T_{max,i} - T_{min,i}} = \frac{T_i - (T_{sp,i} - \frac{\delta_i}{2})}{\delta_i} \quad (8)$$

Now typical thermostat behavior can be described in terms of this normalized parameter instead of individual house temperatures and deadbands:

$$m_i(t) = \begin{cases} 0, & \text{if } \theta_i \leq 0 \\ 1, & \text{if } \theta_i \geq 1 \\ m_i(t^-), & \text{otherwise} \end{cases} \quad (9)$$

Here, a new addition to the thermostat model is proposed which uses the average state of the surrounding units, \tilde{m} , to inhibit operation based on the number of connected units that are operating.

$$m_i(t) = \begin{cases} 0, & \text{if } \theta_i - K_{gain} \tilde{m}_i \leq 0 \\ 1, & \text{if } \theta_i - K_{gain} \tilde{m}_i \geq 1 \\ m_i(t^-), & \text{otherwise} \end{cases} \quad (10)$$

The variable K_{gain} , is a proportional gain to the control feedback introduced. In the simplest term, K_{gain} is a knob that lets the user adjust the effectiveness of the \tilde{m} modification.

The addition of the average ON/OFF state of connected neighbors allows agents to reduce overall demand by causing an earlier entry to the OFF state and a later entry to the ON state, essentially shifting the deadband up, if a larger number of neighbors turn ON. For example, consider a network with $d = 4$, where two of a house's neighbors are ON, resulting in a \tilde{m} of 0.5. Assuming $K_{gain} = 1$, this house will turn OFF as soon as $\theta = 0.5$,

or halfway through the deadband, instead of the standard $\theta = 0$, and won't turn ON until $\theta = 1.5$. With a connection degree of four, each thermostat has the ability to use five upper and five lower bounds depending on the state of neighboring thermostats.

3.2 Extending Model to Multiple Homes in Discrete Time

For ease of simulation, and to more faithfully model the manner in which such a system would be implemented, the first order ODE representing the house dynamics is transformed to the discrete domain (sample time = 1 minute). An arbitrary number of individual agents can then be aggregated into a single Nth order state space model as shown.

$$G(t_{samp}) = e^{\frac{t_{samp}}{RC}} \quad (11)$$

$$H_I(t_{samp}) = (e^{\frac{t_{samp}}{RC}} - I) \quad (12)$$

$$H_{II}(t_{samp}) = (e^{\frac{t_{samp}}{RC}} - I) \left(\frac{Q}{C} \right) \left(\frac{1}{RC} \right)^{-1} \quad (13)$$

Plugging in Equations 11 - 13 into the discrete state space form, the complete equation for the heat transfer dynamics can be seen in Equation 14.

$$T(k+1) = GT(k) + H_I T_\infty + H_{II} m(k) \quad (14)$$

In the forgoing discussion, the state space coefficients (G, H_I, H_{II}) are scalars and k is the discrete time index. To represent N such units, we simply create aggregate matrices with these scalars on the diagonals. The individual units are naturally uncoupled (with the exception that they experience the same ambient temperature). Coupling will be introduced through the peer-to-peer communication and is seen in the m variable. This will be handled in the stability analysis

In the discrete time domain, the modified thermostat behavior is shown in Equation 15. The \tilde{m} variable is computed from the state of adjacent thermostats at the previous sampling period.

$$m_i(k) = \begin{cases} 0, & \text{if } \theta_i(k) - K_{gain} \tilde{m}_i(k-1) \leq 0 \\ 1, & \text{if } \theta_i(k) - K_{gain} \tilde{m}_i(k-1) \geq 1 \\ m_i(k-1), & \text{otherwise} \end{cases} \quad (15)$$

3.3 System Parameters

Parameter values were adopted from the [2] study and are displayed in the Table 1. While populations of homogeneous houses are not entirely realistic, they are a fair approximation for tract house, also referred to as cookie cutter neighborhoods.

While simulating homogeneous houses gives insight to a more severe case, we also model the more realistic case of heterogeneous populations. Heterogeneous houses are simulated to reinforce the result from the homogeneous populations. By confirming results found in the homogeneous populations, this study will test the feasibility of implementing the proposed thermostat modification.

Homes with varying size and construction material are estimated by creating a statistical distribution around the homogeneous values. A parameter spread of $\pm 15\%$ is desired, which results in the normal standard deviations found in Table 1. The values were generated using MATLAB's RANDN() function. The RANDN() function returns a sample of random numbers with a normal distribution based off of a mean and standard deviation provided.

The energy transfer rate of a house's AC unit is sized depending upon the thermal dynamics of the house. The homogeneous population of houses' 14 kW is equivalent to a 4 ton unit (1 ton = 3.5 kW_{th}), which, for these parameters, means that the cooling rate is 0.8 °C/hr, or the temperature moves from the upper limit of the deadband to the lower limit in about 37.5 minutes. The necessary tonnage to achieve this cooling time for the heterogeneous population was calculated and then rounded up to the nearest half-ton to reflect sizes commercially available. The resulting range in unit sizes is 3.5-5 tons (12.25-17.5 kW_{th}). Rounding up of the unit size results in slight over sizing, which means some houses will cooler faster than 37.5 minutes and therefore cycle more often than their homogeneous counterpart. The minimum cooling time for a heterogeneous house is 30.4 minutes.

TABLE 1. Population Parameter Values

Parameter	Value
R , Thermal resistance	2 °C/kW
C , Thermal capacitance	10 kWh/°C
P , Energy transfer rate	14 kW
η , Load efficiency	2.5
T_{sp0} , Initial setpoint temperature	20 °C
T_∞ , Ambient temperature	32 °C
δ , Thermostat deadband	0.2 - 0.5 °C

It should be noted that for the homogeneous populations, the ambient temperature, T_∞ , is kept at a constant 32°C. While this is not

realistic, allows the study to focus on the effect of the input, $m(t)$.

3.4 Simulated Attack

The security of the designed system will be tested by analyzing the effects of failures due to cyber-physical attacks through two parts. The first part being an analysis of the algebraic connectivity of varying populations. The second part of the study will be validating the analysis of the algebraic connectivity by simulating a cyber-physical attack in the agent based model. By comparatively analyzing these two parts, the improvements in security and resilience of the proposed model will be shown.

The simulated attack will show the effects of a loss of communication between neighboring thermostats. This simulated attack could possibly occur from communication jamming or a denial of service attack targeting a communication module. By compromising the peer-to-peer communication, it is effectively setting the \bar{m} value to zero for any attacked thermostat. As mentioned earlier, if the \bar{m} value is set to zero, the thermostat effectively reverts back to the simple thermostat model, which could lead to a dangerous rebound after a DR event.

For the simulation, \bar{m} is calculated through the use of the adjacency matrix of the system. The loss of communication of a thermostat from the population will be modeled by setting the row and column of the corresponding thermostat equal to zero. This act of reverting to the simple thermostat model will be recognized as a failure of the thermostat in the demand response system. Different levels of failure, or differing percent of failed nodes out of the total population, are to be tested. Using a percent of zero failure, or 100% operation, as a baseline, the different levels of failure are tested to the point that demand response is not longer effectively reducing the peak demand of the aggregate system. Baseline simulations will be created at each population, including varying connection architectures.

To compare to the baseline, varying populations are simulated with fixed percentages of total number of houses attacked. The indices of performance used in the previous section are used to represent the systems throughout the simulated attacks. It is to be noted that this test case uses varying numbers of homes. Each simulation starts at an equilibrium point with 42.8% of the house's in an 'On' state and the remaining houses 'Off'. The demand response event occurs at two hours into the simulation and has a duration of 15 minutes.

4 Resilient Design

By further analyzing the graph topology using complex network theory, aligned with graph spectral theory gives the ability to calculate resilience of complex engineered systems [18]. By using these theories to calculate the resilience of a complex system, Mehrpouyan et al. show how design structure can effect the resilience of these systems. This work emphasizes the ability to

use graph theory to show the interconnection of nodes with in a system. The Laplacian matrix.

The Laplacian matrix is defined as:

$$\mathcal{L} = \mathcal{D} - \mathcal{A} \quad (16)$$

Where \mathcal{D} is the degree matrix, or a diagonal $N \times N$ matrix representing the number of connections each node has. The algebraic connectivity, or second smallest eigenvalue of the Laplacian matrix, quantifies the average difficulty to isolate a node from the system. A lower algebraic connectivity is related to a higher level of modularity within the system. Mehrpouyan et al. demonstrated the importance of modularity in a system but is clear to highlight that modularity does not increase the systems tolerance to failure but increases the reliability of the system because of the ability to fix and maintain the system's modules individually [19, 20].

5 Results

The algebraic connectivity was found for varying populations and varying graph construction. These results can be seen in Figure 1.

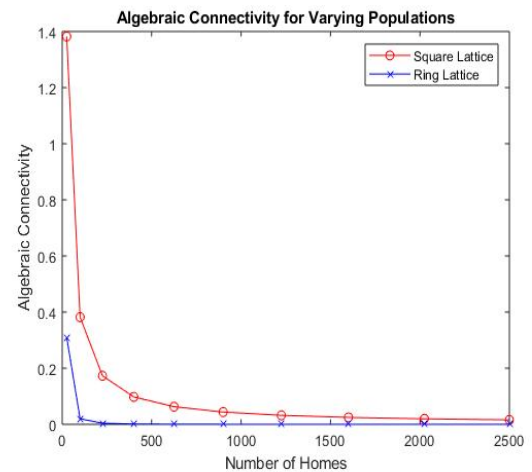


FIGURE 1. Algebraic Connectivity for Varying Populations of Homes.

To test the effect of the resilience of a graph to the desired demand response ability of the population, the simulated nodal attack was completed for varying populations and graph structures. For each simulation percent increase of maximum power is displayed for varying populations, as they experience an attack on 20% of total population. These values are shown on Table 2.

TABLE 2. Percent Increase for Varying Population with 20% Failure (Last M, $\delta = 0.5$)

$\delta = 0.5$ & Last M		
N	Square	Ring
25	14.29%	6.67%
100	13.21%	20.75%
225	12.71%	15.52%
400	13.59%	15.64%
625	15.24%	19.12%
900	14.47%	20.61%
1225	16.94%	15.43%
1600	18.013%	22.06%
2025	18.05%	22.12%
2500	21.83%	21.45%
Avg.	15.84%	17.94%

This process was then repeated for a deadband size of $\delta = 0.2$. The results for the simulated attack on the population with a smaller deadband can be seen in Table 3.

TABLE 3. Percent Increase for Varying Population with 20% Failure (Last M, $\delta = 0.2$)

$\delta = 0.2$ & Last M		
N	Square	Ring
25	10.53%	10.53%
100	12.16%	3.66%
225	9.04%	4.49%
400	7.33%	4.13%
625	5.72%	3.46%
900	3.71%	3.09%
1225	1.75%	2.88%
1600	3.10%	2.83%
2025	4.25%	2.86%
2500	4.46%	2.87%
Avg.	6.20%	4.08%

Each population uses a baseline for maximum power from a simulation with zero houses attacked. For all population with a deadband equal to $\delta = 0.2$ it can be seen that the percent increase for a ring lattice is less than that of a square lattice. As the deadband increases, the simulated response becomes greater removed from the predictions using algebraic connectivity, or simply, the square lattice experiences smaller percent increases of maximum power.

Through the testing of the simulation it was observed that the location of the houses which were attack effected the aggregate demand of the system. This was verified by varying the location of attacked homes on a constant population of 100 homes, connected with a square lattice. Locations chosen for the attacks were the first N number of attacked homes of the population, the last N number of attacked homes in the population, and alternately attacking the first 2N number of attacked homes in the population (i.e. Home 1,3,5...2N). A summary of the effect of varying attack location is shown through percent increase of maximum power. This test focused on a two deadband sizes of $\delta = 0.5$, (shown in Table 4).

TABLE 4. Number of Homes till Failure with Varying Location

Population	Front	Back	Alternating
25	14.3%	7.1%	14.3%
100	13.2%	13.2%	22.6%
225	12.7%	11.9%	26.3%
400	13.6%	11.2%	18.9%
625	15.2%	14.0%	31.1%
900	14.5%	14.5%	18.4%
1225	16.9%	13.5%	32.9%
1600	18.0%	17.2%	22.1%
2025	18.0%	16.7%	37.6%
2500	21.8%	19.9%	24.9%
Average	15.8%	13.9%	24.9%

A summary of all the populations tested for the effects of varying location are shown in Table 5. The values shown are the average percent increase over varying population sizes. An example of this average is shown on the final row of Table 4.

TABLE 5. Summary of Location Effect from Cyber Attacks ($\delta = 0.5$)

%	Front		Back		Alternating	
	Square	Ring	Square	Ring	Square	Ring
10%	6.7%	8.6%	8.5%	8.9%	11.5%	10.6%
20%	15.8%	17.9%	13.9%	16.7%	24.9%	21.1%
30%	26.3%	26.8%	24.8%	27.1%	38.9%	26.4%

6 Resilience Conclusions

The results displayed in Figure 1 clearly shows that both population size and graph structure effect the resilience of a population. Algebraic connectivity was calculated after the simulated attack, presenting a value of zero for each system. An algebraic connectivity of zeros shows that the graph is not connected. This coincides with the simulating an attack to remove the ability to communicate between houses. Algebraic connectivity for as centralized controller was found to be a value of one. This calculated value for the centralized controller was larger than all values, except 25 homes connected with a square lattice, validating the decision to move toward a de-centralized controller.

The ring lattice, for smaller deadband sizes, showed both better algebraic connectivity, as well as a better ability, as a whole, to operate with attacked home. For larger populations and larger percentage of attacked homes the ring lattices saw a smaller percent increase in maximum power.

The simulated attack created failures in communication by altering the adjacency matrix of the graph, setting row and column of the corresponding houses to zero. Slight differences were found when the attacked houses were positioned at the end of the population. When further studied, the location of the attack showed larger differences on the total number of houses to failure. The most vulnerable of the test attacks was attacked at the beginning of the population but alternating every other house.

One reason the attack alternating every other house was the most effective is because it effects more houses in the population. By attacking the houses in a close group, only a few of the houses neighboring the edge houses are effected. However, distributing the attack effects every house connected to the attacked houses.

6.1 Future Work

Showing the comparison between lattice structures shows the dependence of the demand response to the graph as well as shows potential reasoning on using one above the other. Only two simple lattice structures were used for the study, further work testing other lattice structures is needed to find the optimal graph for the proposed criteria. It should be noted the study on the effects of location of attacks was completed only with the square lattice, further testing should be done on all additional lattice structures.

For the study the gain value in the additional criteria was kept at a constant of $K_{gain} = 0.8$. This was chosen because it fall clearly below the stability limit in a parallel study of the stability of the system. Testing the effect of the gain value on the resilience of the system show a great area of interest.

Finally, the study has looked at the ability of the system to function while under an cyber-physical attack. In moving forward in the advancement of the purposed criteria, the ability of the system to self heal is crucial.

ACKNOWLEDGMENT

This work was supported in part by US Department of Energy, DOE-EE0007726 (DOE Industrial Assessment Center) and the Center for Advanced Energy Studies and the National Science Foundation Computer and Information Science and Engineering (CISE), program award number 1846493 of the Secure and Trustworthy Cyberspace (SaTC) program: Formal TOols foR SafEty aNd Security of Industrial Control Systems (FOREN-SICS).

REFERENCES

- [1] Denholm, P., O'Connel, M., Brinkman, G., and Jorgenson, J., 2015. Overgeneration from Solar Energy in California: A Field Guide to the Duck Chart. Tech. Rep. NREL/TP-6A20-65023, National Renewable Energy Laboratory, Nov.
- [2] Callaway, D. S., 2009. "Tapping the energy storage potential in electric loads to deliver load following and regulation, with application to wind energy". *Energy Conversion and Management*, **50**(5), May, pp. 1389–1400.
- [3] Malhame, R., and Chong, C.-Y., 1985. "Electric load model synthesis by diffusion approximation of a high-order hybrid-state stochastic system". *IEEE Transactions on Automatic Control*, **30**(9), Sept., pp. 854–860.
- [4] Xu, Z., Ostergaard, J., Togeby, M., and Marcus-Moller, C., 2007. "Design and Modelling of Thermostatically Controlled Loads as Frequency Controlled Reserve". In 2007 IEEE Power Engineering Society General Meeting, pp. 1–6.
- [5] Bashash, S., and Fathy, H. K., 2013. "Modeling and Control of Aggregate Air Conditioning Loads for Robust Renewable Power Management". *IEEE Transactions on Control Systems Technology*, **21**(4), July, pp. 1318–1327.
- [6] Bashash, S., and Fathy, H. K., 2011. "Modeling and control insights into demand-side energy management through setpoint control of thermostatic loads". In Proceedings of the 2011 American Control Conference, pp. 4546–4553.
- [7] Wood, L. B., and Harry Asada, H., 2011. "Cellular Stochastic Control of the Collective Output of a Class of Distributed Hysteretic Systems". *Journal of Dynamic Systems, Measurement, and Control*, **133**(6), p. 061011.

- [8] Zhang, W., Lian, J., Chang, C. Y., and Kalsi, K., 2013. “Aggregated Modeling and Control of Air Conditioning Loads for Demand Response”. *IEEE Transactions on Power Systems*, **28**(4), Nov., pp. 4655–4664.
- [9] Hao, H., Sanandaji, B. M., Poolla, K., and Vincent, T. L., 2015. “Aggregate Flexibility of Thermostatically Controlled Loads”. *IEEE Transactions on Power Systems*, **30**(1), Jan., pp. 189–198.
- [10] Ramchurn, S. D., Vytelingum, P., Rogers, A., and Jennings, N. “Agent-Based Control for Decentralised Demand Side Management in the Smart Grid”. p. 8.
- [11] Xydas, E., Marmaras, C., and Cipcigan, L. M., 2016. “A multi-agent based scheduling algorithm for adaptive electric vehicles charging”. *Applied Energy*, **177**, Sept., pp. 354–365.
- [12] Lee, R. M., Assante, M. j., and Conway, T., 2016. “Analysis of the Cyber Attack on the Ukrainian Power Grid”. *EISAC*, Mar.
- [13] , 2012. What Is Security and Resilience?, Dec.
- [14] Rothrock, R. Security vs. resilience: Know the difference.
- [15] Rieger, C., Zhu, Q., and Basar, T., 2012. “Agent-based cyber control strategy design for resilient control systems: Concepts, architecture and methodologies”. In 2012 5th International Symposium on Resilient Control Systems, IEEE, pp. 40–47.
- [16] Haimes, Y. Y., Crowther, K., and Horowitz, B. M., 2008. “Homeland security preparedness: Balancing protection with resilience in emergent systems”. *Systems Engineering*, **11**(4), Dec., pp. 287–308.
- [17] Al-Fuqaha, A., Guizani, M., Mohammadi, M., Aledhari, M., and Ayyash, M., 2015. “Internet of Things: A Survey on Enabling Technologies, Protocols, and Applications”. *IEEE Communications Surveys Tutorials*, **17**(4), pp. 2347–2376.
- [18] Mehrpouyan, H., Haley, B., Dong, A., Tumer, I. Y., and Hoyle, C., 2013. “Resilient design of complex engineered systems against cascading failure”. In ASME 2013 International Mechanical Engineering Congress and Exposition, American Society of Mechanical Engineers, pp. V012T13A063–V012T13A063.
- [19] Mehrpouyan, H., Haley, B., Dong, A., Tumer, I. Y., and Hoyle, C., 2015. “Resiliency analysis for complex engineered system design”. *AI EDAM*, **29**(1), pp. 93–108.
- [20] Mehrpouyan, H., Haley, B., Dong, A., Tumer, I. Y., and Hoyle, C., 2013. “Resilient design of complex engineered systems”. In ASME 2013 International Design Engineering Technical Conferences and Computers and Information in Engineering Conference, American Society of Mechanical Engineers, pp. V03AT03A048–V03AT03A048.